PROCEEDINGS OF SCIENCE

Highlights of nucleon decay searches at JUNO

Yuyi Wang[a,*] and Benda Xu[a] on behalf of the JUNO Collaboration

[a] *Department of Engineering Physics & Center for High Energy Physics, Tsinghua University, Beijing, China*

E-mail: wangyy21@mails.tsinghua.edu.cn

We foresee JUNO to be the world's largest liquid-scintillator detector of 20 kton upon its completion, with unprecedented light yield and photo-coverage. JUNO provides us an excellent equipment to search for nucleon decay in parallel to its rich neutrino program, particularly via the decay channels predicted by the supersymmetric unified theories. The particle identification capability of JUNO is the key to tag the cascaded decays and de-excitations. I shall highlight the activities in nucleon decay searches at JUNO with the anticipation of the first data.

42nd International Conference on High Energy Physics (ICHEP2024)
18-24 July 2024
Prague, Czech Republic

∗Speaker

PoS(ICHEP2024)175

1. Introduction

Proton decay is an important prediction of Supersymmetry Grand Unified Theories (SUSY-GUTs). The smoking gun of SUSY over classical GUTs is that $p \to \bar{\nu}K^+$ dominates $p \to e^+\pi^0$. Many SU(5) SUSY-GUTs predicts $p \to \bar{\nu}K^+$, and Super-Kamiokande (SK) has given the lower limit of partial lifetime. The limit is 5.9×10^{33} year in 2014 and 8.2×10^{33} year in 2019 [1, 2]. Some SU(5) SUSY-GUTs have been ruled out, *e.g.*, minimal SUSY SU(5) predicts 10^{28} year to 10^{32} year [3]. Some of them are still possible, *e.g.*, SUGRA SU(5) predicts 10^{32} year to 10^{34} year, while SUSY SU(5) in 5D predicts 10^{34} year to 10^{35} year [3]. Therefore, the limitation given by experiments should reach 10^{35} year scale to prove them.

The detection of $p \to \bar{\nu}K^+$ is focused on K^+ because the energy of $\bar{\nu}$ is low, and $\bar{\nu}$ is invisible in detectors. K^+ mainly follows 2 decay paths. The first one is $K^+ \to \mu^+\nu_\mu$, while μ^+ decays into a Michel electron afterwards. The second one is $K^+ \to \pi^+\pi^0$. π^0 has a short lifetime (84.3 ± 1.3) as, and decays into 2γ very fast. π^+ decays into a muon: $\pi^+ \to \mu^+\nu_\mu$. Therefore, the decay of K^+ could be divided into 3 parts: the signal of K^+ itself, the decay daughters and the Michel electrons. Figure 1 shows a simulated histogram of the three signals.

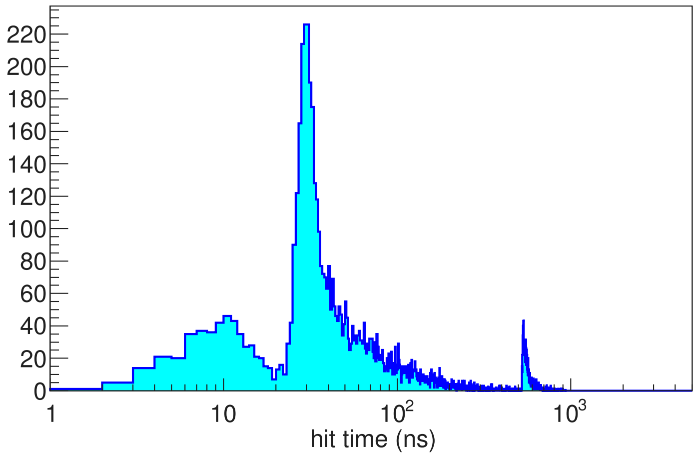

Figure 1: The time signature of K^+ [4].

In a water Cherenkov detector, K^+ is below the threshold and invisible; so is the μ^+ produced by π^+. SK uses the γ ray from ^{15}N de-excitation to indentify K^+ [1]. Undagoitia et al. investigated that liquid scintillator is ideal for identifying K^+ [5]. The idea was realized by KamLAND in 2015, which gave a result of 5.4×10^{32} year partial lifetime [6].

2. Sensitivity of JUNO on proton decay

2.1 JUNO experiment

Jiangmen Underground Neutrino Observatory (JUNO) is a large liquid scintillator (LS) detector to be online, shown in Figure 2. The center detector is a 20 kt LS acrylic container, covered by 17612 20-inch photomultiplier tubes (PMTs) and 25600 3-inch PMTs. The PMTs cover 78 % of the LS sphere. The 3-inch PMTs feature a larger dynamic range without saturation, making them suitable for K^+ detection, as its energy is mainly 0.5 GeV. Figure 3 shows the relative position of the PMTs in different sizes.

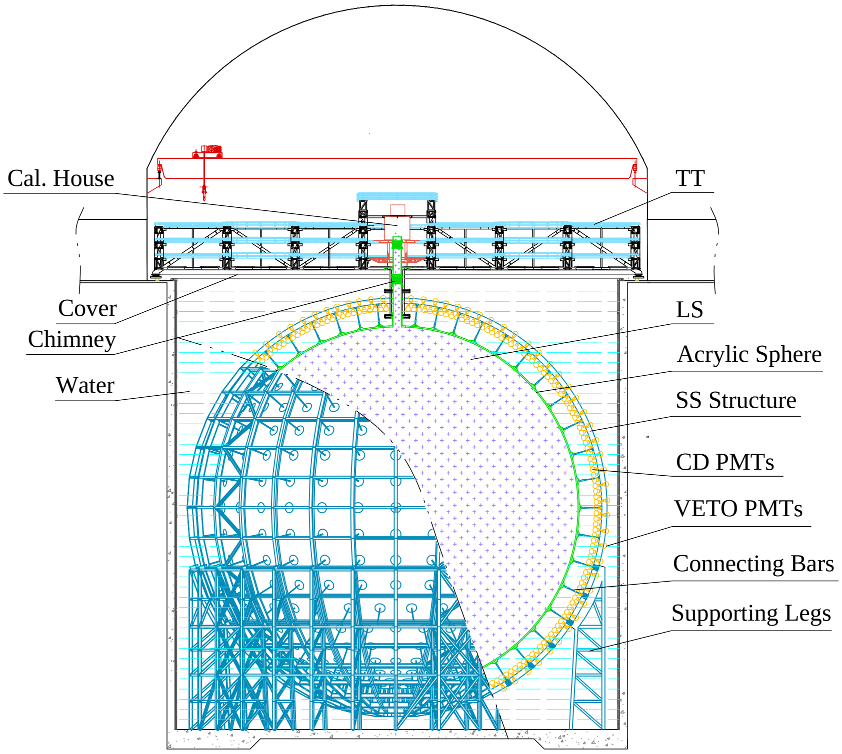

Figure 2: The structure of JUNO [7].

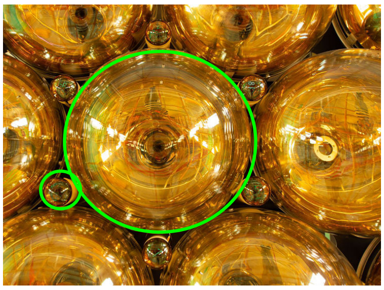

Figure 3: The 20-inch PMTs and the 3-inch PMTs.

2.2 Atmospheric neutrino background

The vertex reconstruction is achieved by fitting multiple pulses on 3-inch PMT hits, incorporating photon time-of-flight correction. The rising edge is found at the residual time histogram. Figure 4a shows a K^+ hit time histogram fit with double-pulse $K - \mu$ template. Figure 4b shows the fit on an atmospheric neutrino signal, which is the most important background of proton decay. To avoid degeneracy, a minimal separation of 7 ns between two pulses is required. The hypotheses are discriminated by χ^2 ratios.

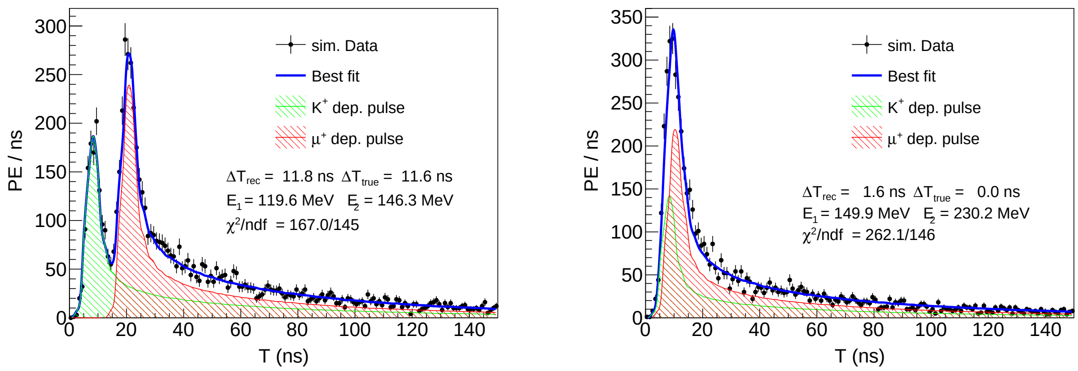

(a) Double-pulse fit of a K^+ signal. **(b)** Double-pulse fit of an atmospheric neutrino signal.

Figure 4: Double-pulse fit of different signals [8].

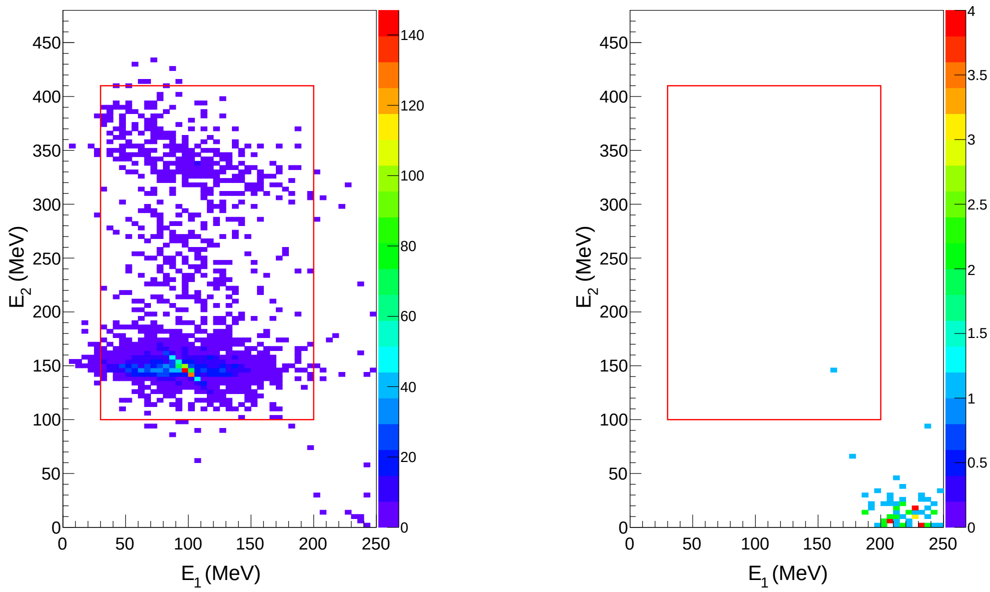

(a) The K^+ signal. **(b)** The atmospheric neutrino signal.

Figure 5: Histogram of energy of first pulse E_1 and the second pulse E_2, for different kind of signals [8].

The double-pulse fit results in the energy of the first pulse E_1 and the second pulse E_2. The scatter plot of the individual pulse energies in Figure 5 is different for K^+ signal and atmospheric neutrino signal. In Figure 5a, two decay modes of K^+ construct the two clusters in the histogram. The upper one is $K^+ \to \pi^+ + \pi^0$. The lower one is $K^+ \to \mu^+ + \nu_\mu$, which is the most possible decay mode. In the μ^+ decay mode, some of the energy is carried by an invisible ν_μ, thus E_2 is lower. In Figure 5b, atmospheric neutrino signals produce single pulse, so E_2 is small. Therefore, the events outside the red box are rejected as background.

2.3 Simulation setup

The sensitivity study is powered by simulation. The atmospheric neutrino events are generated by GENIE 3.0.2 [9], with final state interaction taken into account. The K^+ is generated by a customized GENIE. It considers nuclear shell structure, and calculates proton mass considering binding energy. The hadron-nucleon model is also turned on, for $K^+n \to K^0p$ interaction. The customized GENIE is also used to generate excited energy spectrum of residual nuclei. TALYS 1.95 [10] with excited energy spectrum is used as input to handle de-excitations.

In the detector response simulation, SNiPER [11], a JUNO-customized Geant4 [12] is used for energy deposition and scintillation optics. K^+ and atmospheric neutrino are uniformly distributed in the LS sphere in the simulation.

2.4 Evolution of the efficiency

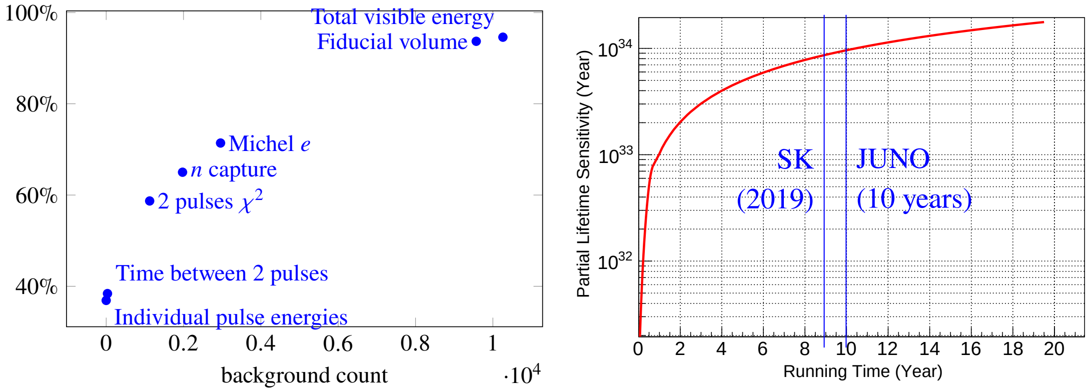

(a) The evolution of detection efficiency and background count. From right to left.

(b) The predicted sensitivity of JUNO by the running time. SK result in 2019 is also marked on the plot [8].

Figure 6: The sensitive study result of JUNO for $p \to \bar{\nu}K^+$.

Figure 6a shows the evolution of the detection efficiency, applying each cut methods. It finally gives 36.9 % efficiency for background level 0.2. For comparison, the efficiency of KamLAND in 2015 is 44 % [6]. KamLAND gives better detection efficiency because JUNO is larger and requires the cut to be more stringent. Compared to SK, JUNO as an LS detector has advantages: SK searches signals by prompt de-exitation γ at 9.1 % efficiency, $\pi^+\pi^0$ at 10 % efficiency and mono-energetic muon with background [1].

As shown in Figure 6b, the sensitivity increases by the time, and scales linearly with exposure because it is a background-free search. After 10 years, the exposure of JUNO will be 200 kt · year, and the lower limit of partial lifetime will be 0.96×10^{34} year at 90 % confidence level [4].

2.5 Future developments

The research depends on the $K - \pi$ and $K - \mu$ templates. It could be more sensitive to event locations directions with careful calibration. A Bayesian model could be used to distinguish single pulse and double pulses, instead of a constant time difference of the two fitted pulses. The sensitivity research uses only the hit time from 3-inch PMTs, because the number of PE hit on the 20-inch PMTs could be easily larger than one, causing pile-up and saturation. Figure 7a shows the difference of the waveforms from the two kinds of PMTs. To solve the problem, a waveform analysis method based on FSMP [13] could be applied.

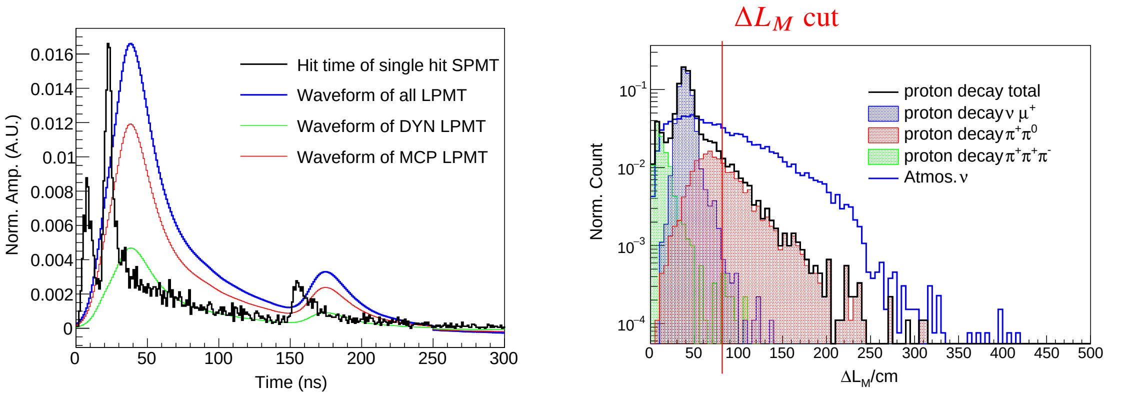

(a) The waveforms of 3-inch PMT (SPMT) and 20-inch PMT (LPMT).

(b) The normalized count distribution of ΔL_M of different events.

Figure 7: Characteristics of the simulation data [8].

The selection based on reconstruction of muon and Michel electrons also decreases the detection efficiency in a large scale. In the sensitivity study, define the tagged Michel electron number as N_M and the correlated distance as ΔL_M. N_M should be 1 or 2, while $\Delta L_M \leq 80\,\text{cm}$. Figure 7b shows the distribution of ΔL_M and the cut, which reduces many $K^+ \to \pi^+\pi^0$ events. To improve the efficiency, multi-point and segment reconstruction for muon and multiple Michel electrons should be developed.

3. Ongoing study: invisible neutron decay

There is an ongoing study in JUNO on invisible decay modes of neutrons [8]. The neutron in ^{12}C may decay in two invisible modes: $n \to \text{inv}$ ($^{12}\text{C} \to {}^{11}\text{C}^*$) and $nn \to \text{inv}$ ($^{12}\text{C} \to {}^{10}\text{C}^*$). The decay products are invisible, so the detection focus on the de-excitation products of $^{11}\text{C}^*$ and $^{10}\text{C}^*$. Some de-excitation modes of the excited residual nuclei can produce a triple coincidence signal [8]. The study shows that the sensitivity of 10 years data taking of each decay mode is $\tau/B(n \to \text{inv}) > 5.0 \times 10^{31}$ year at 26.7 % efficiency, and $\tau/B(nn \to \text{inv}) > 1.4 \times 10^{32}$ year at 42.3 % efficiency.

4. Summary

While some of SU(5) SUSY-GUTs are still viable, $p \to \bar{\nu}K^+$ is still the most interesting process predicted. Liquid scintillators are ideal to identify K^+ is this prediction and measure its energy. There are other nucleon decay searches at JUNO, *e.g.*, invisible neutron decay $n \to \text{inv}$ and $nn \to \text{inv}$. After 10 years of data taking, the expected sensitivities at 90 % confidence level are $\tau/B(p \to \bar{\nu}K^+) > 0.96 \times 10^{34}$ year, $\tau/B(n \to \text{inv}) > 5.0 \times 10^{31}$ year and $\tau/B(nn \to \text{inv}) > 1.4 \times 10^{32}$ year.

References

[1] Super-Kamiokande Collaboration, K. Abe, Y. Hayato, K. Iyogi, J. Kameda, M. Miura et al., *Search for proton decay via $p \to \nu K^+$ using* 260 kiloton · year *data of Super-Kamiokande*, *Physical Review D* **90** (2014) 072005.

[2] A. Takenaka, "Search for Proton Decay: The Latest Results from Super-Kamiokande." NuPhys2019, 2019.

[3] P.S.B. Dev, L.W. Koerner, S. Saad, S. Antusch, M. Askins, K.S. Babu et al., *Searches for baryon number violation in neutrino experiments: a white paper*, *Journal of Physics G: Nuclear and Particle Physics* **51** (2024) 033001.

[4] A. Abusleme, T. Adam, S. Ahmad, R. Ahmed, S. Aiello, M. Akram et al., *JUNO sensitivity on proton decay $p \to \nu K^+$ searches*, *Chinese Physics C* **47** (2023) 113002.

[5] T.M. Undagoitia, F. von Feilitzsch, M. Göger-Neff, C. Grieb, K.A. Hochmuth, L. Oberauer et al., *Search for the proton decay $p \to K^+\bar{\nu}$ in the large liquid scintillator low energy neutrino astronomy detector LENA*, *Physical Review D* **72** (2005) 075014.

[6] K. Asakura, A. Gando, Y. Gando, T. Hachiya, S. Hayashida, H. Ikeda et al., *Search for the proton decay mode $p \to \bar{\nu}k^+$ with KamLAND*, *Physical Review D* **92** (2015) 052006.

[7] *JUNO physics and detector*, *Progress in Particle and Nuclear Physics* **123** (2022) 103927.

[8] J. Collaboration, A. Abusleme, T. Adam, K. Adamowicz, S. Ahmad, R. Ahmed et al., *JUNO Sensitivity to Invisible Decay Modes of Neutrons*, 2024.

[9] C. Andreopoulos, C. Barry, S. Dytman, H. Gallagher, T. Golan, R. Hatcher et al., *The genie neutrino monte carlo generator: Physics and user manual*, 2015.

[10] A. Koning and D. Rochman, *Modern nuclear data evaluation with the talys code system*, *Nuclear Data Sheets* **113** (2012) 2841.

[11] J.H. Zou, X.T. Huang, W.D. Li, T. Lin, T. Li, K. Zhang et al., *SNiPER: an offline software framework for non-collider physics experiments*, *Journal of Physics: Conference Series* **664** (2015) 072053.

[12] S. Agostinelli, J. Allison, K. Amako, J. Apostolakis, H. Araujo, P. Arce et al., *Geant4—a simulation toolkit*, *Nuclear Instruments and Methods in Physics Research Section A: Accelerators, Spectrometers, Detectors and Associated Equipment* **506** (2003) 250.

[13] Y. Wang, A. Zhang, Y. Wu, B. Xu, J. Chen, Z. Wang et al., *The Fast Stochastic Matching Pursuit for Neutrino and Dark Matter Experiments*, 2024.